The Astrophysical Journal, 689:194–202, 2008 December 10

THE MAGELLANIC CLOUD CALIBRATION OF THE GALACTIC PLANETARY NEBULA DISTANCE SCALE

Letizia Stanghellini and Richard A. Shaw
National Optical Astronomy Observatory, 950 North Cherry Avenue, Tucson, AZ 85719; lstanghellini@noao.edu, shaw@noao.edu

and

Eva Villaver[1]
Space Telescope Science Institute, 3800 San Martin Drive, Baltimore, MD 21218; villaver@stsci.edu
Received 2008 January 14; accepted 2008 June 17

ABSTRACT

Galactic planetary nebula (PN) distances are derived, except in a small number of cases, through the calibration of statistical properties of PNs. Such calibrations are limited by the accuracy of individual PN distances, which are obtained with several nonhomogeneous methods, each carrying its own set of liabilities. In this paper we use the physical properties of the PNs in the Magellanic Clouds and their accurately known distances to recalibrate the Shklovsky/Daub distance technique. Our new calibration is very similar (within 1%) to the commonly used distance scale by Cahn et al., although there are important differences. We find that neither distance scale works well for PNs with classic ("butterfly") bipolar morphology, and while the radiation-bounded PN sequences in both the Galactic and the Magellanic Cloud calibration have similar slopes, the transition from optically thick to optically thin appears to occur at higher surface brightness and smaller size than in that adopted by Cahn et al. The dispersion in the determination of the scale factor suggests that PN distances derived by this method are uncertain by at least 30%, and that this dispersion cannot be reduced significantly by using better calibrators. We present a catalog of Galactic PN distances using our recalibration, which can be used for future applications, and compare the best individual Galactic PN distances to our new and several other distance scales, both in the literature and newly recalibrated by us, finding that our scale is the most reliable to date.

Subject heading: planetary nebulae: general

Online material: machine-readable table

1. INTRODUCTION

The uncertainty associated with distance measurements of Galactic planetary nebulae (PNs) is a major obstacle to the advancement of PN research. Only ~40 Galactic PNs have distances that have been determined individually with reasonable accuracy. Distances to Galactic PNs can be determined individually in various ways, including cluster membership (Chen et al. 2003, hereafter CHW03; Alves et al. 2000, hereafter ABL00), by measuring the rate of their expansion (e.g., Liller & Liller 1968, hereafter LL68; Hajian et al. 1995, hereafter HTB95), by the reddening method (e.g., Gathier et al. 1986, hereafter GPP86; Kaler & Lutz 1985, hereafter KL85), and by measuring their spectroscopic parallax (Ciardullo et al. 1999, hereafter C99) or trigonometric parallax (Harris et al. 2007, hereafter H07).

For the remaining >1800 Galactic PNs (Acker et al. 1992) one has to rely on statistical distance scales, whose calibrations are based on the reliability of the individually known PN distances, and the validity of a general correlation that links the distance-dependent to the distance-independent physical properties of PNs. The Cahn et al. (1992, hereafter CKS) distance scale of Galactic PNs is based on an attempt by Daub (1982, hereafter D82) to improve Shklovsky's distance scale (Shklovsky 1956a, 1956b) for optically thick nebulae. Shklovsky's distance scale assumes that all PNs have equal (observed) ionized mass. D82 assumed that Shklovsky's constant mass approach was still valid, but only for those PNs that are optically thin to the Lyman continuum radiation emitted by the central stars (density bounded). For the optically thick (radiation bounded) PNs, D82 based the distance scale on a calibration of an ionized mass versus surface brightness relation. CKS improved D82's calibration with the use of a larger number of calibrators (PNs with known individual distance) and calculated the statistical distances to 778 Galactic PNs.

Since publication of the CKS catalog, these distances have been used preferentially and widely in the literature. Other statistical methods that have been commonly used include those by Maciel (1984), Zhang (1995, hereafter Z95), van de Steene & Zijlstra (1995, hereafter vdSZ95), Schneider & Buckley (1996, hereafter SB96), and Bensby & Lundström (2001, hereafter BL01). All these distance scales rely on a set of Galactic calibrators whose distances are mostly derived from reddening or expansion properties, or from the assumption of Galactic bulge membership, with all the consequent uncertainties. With the publication over the past decade of critical physical parameters for a large sample of Magellanic Cloud PNs (Shaw et al. 2001, 2006; Stanghellini et al. 2002, 2003), including highly accurate Hβ fluxes, physical dimensions, morphologies, and extinction constants, we have the opportunity to assess and improve the distance scale for Galactic PNs. In this paper we take advantage of the wealth of Magellanic Cloud PN data to recalibrate the CKS distance scale, as well as other distance scales for comparison. Homogeneously determined photometric radii from the *Hubble Space Telescope* (*HST*) of a PN sample with low Galactic reddening are the best way to determine any relation that involves apparent diameters. Furthermore, the relatively recent publication of trigonometric and spectroscopic

[1] Affiliated with the *Hubble Space Telescope* Division of the European Space Agency.

parallax and cluster membership distances to Galactic PNs allows us to test with unprecedented reliability our own and other distance scales.

The construction of any statistical distance scale for PNs is composed of three fundamental steps: the selection of a *method* that has some physical or empirical basis, the selection of a set of *calibrator PNs*, for which distances have been determined by some independent means, and an analysis of the *applicability* of the calibration to a wide variety of PNs. Until now it has been difficult to compare the viability of various methods, since their calibrations and applications have varied so widely. In § 2 we describe in detail the Shklovsky/Daub/CKS distance scale and the superiority of the Magellanic Cloud PNs as calibrators. We also derive our new calibration of this method and assess its inherent uncertainties. In § 3 we discuss the physical underpinning of the CKS distance method in light of recent advances in modeling the evolution of PNs. In § 4 we take a closer look at the viability of various methods for determining independent distances to Galactic PNs (i.e., the set that had previously been used as calibrators) and discuss the applicability of the Magellanic Cloud distance scale to Galactic PNs. In § 5 we recalibrate the most used statistical distance methods with the Magellanic Cloud PNs and then compare the accuracy of these methods to one another using the best independently determined distances to Galactic PNs. We conclude in § 6 with our final prescription and recommendation for determining statistical distances to Galactic PNs.

2. THE MAGELLANIC CLOUD CALIBRATION AND THE NEW PN DISTANCE CATALOG

The CKS statistical distance scale is based on the calibration of the relation between D82's ionized mass,

$$\mu = \left(2.266 \times 10^{-21} D^5 \theta^3 F\right)^{1/2}, \tag{1}$$

and the optical thickness parameter,

$$\tau = \log\left(\frac{4\theta^2}{F}\right), \tag{2}$$

where D is the distance to the PN in parsecs, θ is the nebular radius in arcseconds, and F is the nebular flux at 5 GHz. The parameter μ increases as the ionization front expands into the nebula. Once a PN becomes density bounded, μ remains constant for the rest of the observable PN lifetime.

By calculating μ and τ for several PNs with known distances, dimensions, and fluxes, CKS derived the μ-τ relation:

$$\log \mu = \tau - 4, \quad \tau < 3.13, \tag{3a}$$

$$\log \mu = -0.87, \quad \tau > 3.13, \tag{3b}$$

where equation (3a) holds for PNs of high surface brightness, and equation (3b) for PNs with low surface brightness.

The calibration of the above distance scale was based on 19 Galactic PNs with independent distances with comparatively poor accuracy. At the time when the CKS paper was written there were hardly any Magellanic Cloud PNs with accurately measured diameters, and the distances to the Magellanic Clouds were also quite uncertain. We can now recalibrate the distance scale using the nebular parameters relative to the LMC and SMC PNs observed by us with *HST* (Shaw et al. 2001, 2006; Stanghellini et al. 2002, 2003). In order to determine τ and μ for Magellanic Cloud PNs we use a transformation between the 5 GHz and the Hβ fluxes (eq. [6] in CKS), since radio fluxes are not available for Magellanic Cloud PNs. All other parameters are available in our *HST* paper series. Note that we use the photometric radius as the proper measure of the nebular dimension, which is defined as the radius that includes 85% of the flux in a monochromatic emission line.

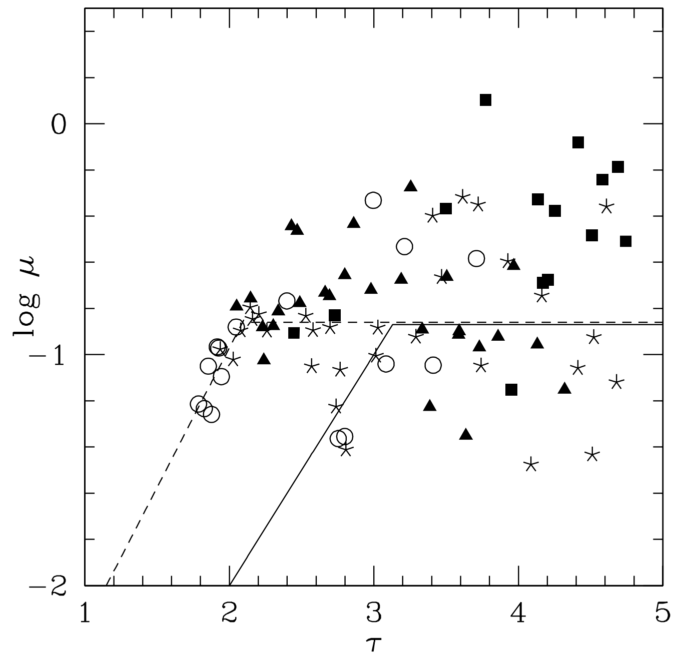

Fig. 1.—Plot of log μ vs. τ for the sample of LMC PNs observed with *HST.* Symbols indicate morphology types: round (*open circles*), elliptical (*asterisks*), bipolar core (*triangles*), and bipolar (squares). The thinning sequence is clearly defined for $\tau < 2.1$. The solid line shows the CKS calibration, and the dashed line shows the new calibration (SSV).

We have adopted a distance to the LMC of 50.6 kpc (Freedman et al. 2001; Mould et al. 2000), which is accurate to ~10% (Benedict et al. 2002). The variation in the adopted distance when applied to individual objects can be easily estimated given that the three-dimensional structure (3D) of the LMC has been well established (Freeman et al. 1983; van der Marel & Cioni 2001). The LMC can be considered a flattened disk with a tilt of the LMC plane to the plane of the sky of 34° (van der Marel & Cioni 2001). Freeman et al. (1983) derived a scale height of 500 pc for an old disk population. The scale height of young objects is between 100 and 300 pc (Feast 1989). If we use the scale height of an old disk population, then the 3D structure of the LMC introduces a variation in the adopted distance that is smaller than 1% from object to object, and therefore it has been neglected in the calibration.

For the SMC we have used a distance of 58.3 kpc (Westerlund 1997). The accuracy of this distance is not as well established as for the LMC. Moreover, the SMC is irregular with a large intrinsic line-of-sight depth (between 6 and 12 kpc; Crowl et al. 2001) which varies with the location within the galaxy. We have estimated an average line-of-sight depth of 5 kpc for the PNs in our sample by combining the span of the positions (400 pc in right ascension and 2 kpc in declination) of the PNs with respect to the optical center of the SMC with the dispersion in the distance to the SMC derived by Crowl et al. (2001) using SMC cluster positions. The distance uncertainty introduced by this depth in the SMC is roughly 9%, still too low to significantly affect the result but one order of magnitude larger than that obtained for the LMC. In this respect we consider LMC PNs to be better calibrators than the SMC PNs for the distance scale.

In Figure 1 we show the LMC PNs on the log μ–τ plane. We have calculated τ and log μ as explained above and assumed

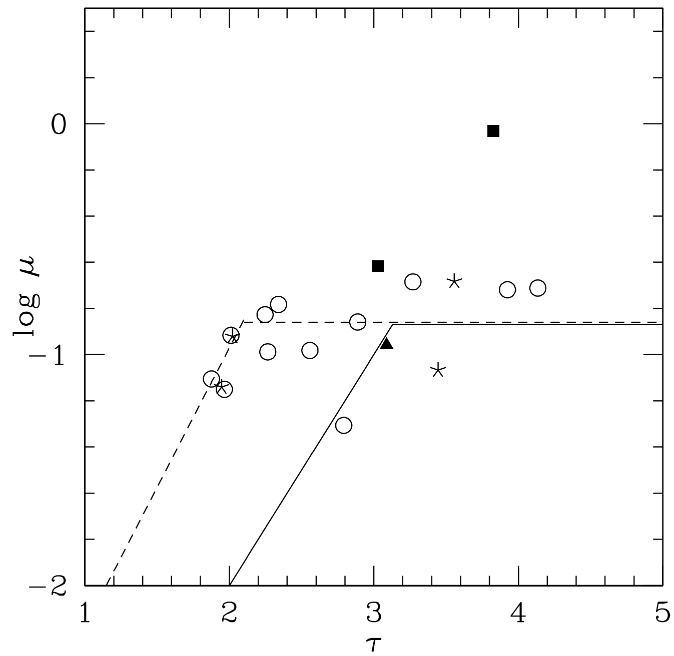

FIG. 2.—Same as Fig. 1, but for the SMC PNs.

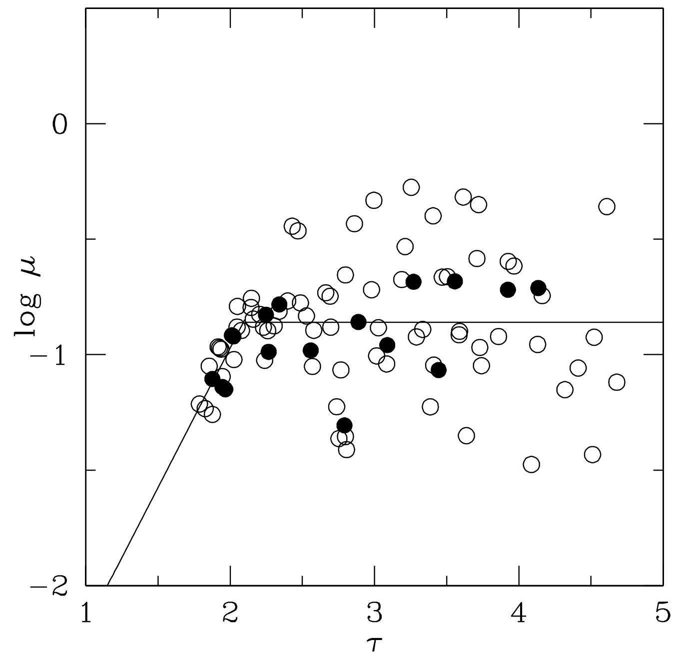

FIG. 3.—LMC (*open circles*) and SMC (*filled circles*) PNs; all morphologies except bipolar PNs are plotted. Our new calibration is plotted as a solid line.

$D_{\rm LMC} = 50.6$ kpc. In the figure we plot the different morphological types with different symbols, following the classification in Shaw et al. (2001, 2006). To guide the eye we have plotted, on the figure, the Galactic distance scale fit from CKS (*solid line*). The optically thick sequence of LMC PNs is very tight for $\tau < 2.1$, and most LMC PNs are optically thin for $\tau > 2.1$. The fitted value of the function for optically thin LMC PNs is almost identical to that of Galactic PNs *if we exclude bipolar planetary nebulae*. The dashed line in Figure 1 corresponds to the Magellanic Cloud fit of the optically thick sequence of LMC PNs (see eqs. [4a] and [4b] below). Similarly, in Figure 2 we show the same plot as in Figure 1, but for SMC PNs. The morphology and sizes of the nebulae are from Stanghellini et al. (2003). Even with the scarcity of data points, the thick PN sequence is well defined by SMC PNs, and it is identical to that of the LMC PNs.

The observed ionized masses of bipolar PNs in both Figures 1 and 2 appear mostly well above the constant ionized mass line. The parameters μ and τ have been calculated with the photometric radii of the PNs, which can be very different from the isophotal radii in the case of PNs with large lobes. Furthermore, bipolar PNs might be optically thick for most of their observed lifetime (Villaver et al. 2002a) and thus are not the ideal calibrators for the optically thin PN branch of the log μ–τ relation. In deriving the distance scale based on Magellanic Cloud PNs we thus exclude PNs with bipolar morphology. This leave us with 70 Magellanic Cloud calibrators, a very large number of PNs with individual distances when compared to the 19 calibrators in CKS. In Figure 3 we show the Magellanic Cloud calibration of the PN distance scale, where open circles are LMC PNs and filled circles are SMC PNs, and where we exclude bipolar PNs. Note that we have assumed that the ionized mass for optically thin PNs is constant, as in D82 and CKS.

The fit to the distance scale based on the Magellanic Cloud PNs (this paper, hereafter SSV) is:

$$\log \mu = 1.21\tau - 3.39, \quad \tau < 2.1, \tag{4a}$$

$$\log \mu = -0.86, \quad \tau > 2.1. \tag{4b}$$

The line in Figure 3 shows this relation. The separation between optically thick and thin PNs is very obvious from the figure, and the optically thick sequence is much better defined here than in CKS, thanks to the use of the best calibrators available now. The optically thick sequence has been derived by least-squares fit and has correlation coefficient $R_{xy} = 0.8$. The optically thin sequence is determined by the average of log μ for $\tau > 2.1$. Using another estimate of the central tendency will change the horizontal scale by less than 5%, which is well within the uncertainty. Furthermore, if we were to fit the data points of Figure 3 with just one line for all τ we would have a very poor correlation ($R_{xy} = 0.14$), which reinforces the evolutionary scheme of optically thick to thin PNs, proposed by D82 to improve Shklovsky's method.

By examining Figure 3 we infer the following: (1) Our analysis allows us to confirm the CKS distance scale for optically thin PNs. (2) The optically thick sequence is very well defined by the Magellanic Cloud PNs and is different from that of CKS. (3) The new statistical distance for optically thin PNs increases slightly the assumed ionized mass, such that distances for optically thin nebulae are typically 1% larger compared to those computed using the CKS calibration. (4) Bipolar PNs do not follow the empirical relation, and their ionized mass actually increases steadily with τ, confirming that they stay in the ionization bound state for much longer than PNs with other morphological types. The probable reason that the bipolar PN relation does not flatten out for $\tau > 2.1$ is that bipolar PNs are the progeny of the more massive stars and are expected to remain optically thick (given a combination of the large circumstellar densities and fast evolution of the central star).

By using the SSV distance scale we calculated the statistical distances to all non-bipolar PNs in the LMC and the SMC. We obtain distributions that are nicely narrow, with mean values (and dispersions) $D_{\rm LMC} = 50.0 \pm 7.5$ kpc and $D_{\rm SMC} = 57.5 \pm 5.5$ kpc, which are within 1% of the distances to the Magellanic Clouds.

We applied our new distance scale to the large sample of Galactic PNs in the original CKS catalog and present the revised distances in Table 1. Column (1) gives the usual name as in CKS, column (2) gives the calculated τ, columns (3) and (4) give the

TABLE 1
CATALOG OF GALACTIC PN DISTANCES

Name (1)	τ (2)	θ (arcsec) (3)	F^{a} (4)	D_{SSV} (pc) (5)
NGC 40	3.46	18.20	0.460	1249
NGC 246	5.31	112.00	0.248	475
NGC 650	5.24	69.20	0.110	746
NGC 1360	5.82	192.00	0.222	351
NGC 1501	4.08	25.90	0.224	1167
NGC 1514	4.59	50.20	0.262	760
NGC 1535	3.31	9.20	0.166	2305
NGC 2022	3.62	9.70	0.091	2518
NGC 2346	4.54	27.30	0.086	1369
NGC 2371	4.33	21.80	0.090	1554

NOTE.—Table 1 is published in its entirety in the electronic edition of the *Astrophysical Journal*. A portion is shown here for guidance regarding its form and content.
[a] This is the 5 GHz flux when available, otherwise the equivalent 5 GHz flux from Hβ.

angular radius and the flux used in the calculation, and column (5) gives the distance to the PNs. Note that the fluxes in column (4) are either the 5 GHz fluxes from CKS, when available, or their Hβ equivalents.

3. THE PHYSICS OF THE STATISTICAL DISTANCE SCALE

As CKS pointed out, the assumption of constant ionized mass for optically thin PNs (or that it can be computed for optically thick PNs with a one-parameter model) would seem to be a doubtful proposition since the progenitor stars vary in mass by nearly an order of magnitude. CKS minimized the significance of the variation in ionized mass by pointing out that distances so derived depend only on the square root of the assumed mass. One might also expect that the ionized mass would be fairly directly correlated with the progenitor mass. However, hydrodynamical models of the coevolving PN and central star by Villaver et al. (2002a) show that the decline of gas density with radius is generally quite steep (except within the bright inner shell of gas) over a wide range of progenitor masses and during the entire visible lifetime of the nebula. The implication is that, for optically thin nebulae, the bulk of the mass exists in the faint, low-density, outer halo. Since the volume emissivity of recombination lines is proportional to the square of the gas density, the massive nebular halo contributes very little to the observed emission. Most published values for PN masses assume a constant density for the gas, one that is only representative of the bright inner shell, leaving the bulk of the PN mass unaccounted for. In part for these reasons, ionized masses derived in this way reflect only a modest fraction of the total mass of the nebula, such that the assumption of a constant mass is sufficiently accurate to render the Shklovsky distance method useful.

We have shown that the distance method of CKS is empirically sound and derived the scale factor for optically thin PNs to that from observations of Magellanic Cloud PNs. It is important to note the significance of the *dispersion* in the PN masses (expressed in the μ parameter) about the mean in the calibration shown in Figure 3. The 1 σ deviation about the mean value is 0.28, which translates to a corresponding uncertainty in the distance of about 30%. We regard this value as a rough estimate of the minimum uncertainty that may be associated with the distance to an individual PN derived using this methodology. It is important to note that the uncertainty in the distance scale *cannot* be reduced with improved calibrator nebulae, since the distance uncertainty is of the order of 10% (i.e., of the order of the size of the circles in Fig. 3). The scatter in the data results from genuine variations in the ionized masses of the calibrator nebulae and quantifies the fundamental limitation in this technique.

The new PN distance scale (SSV) is very similar to that of CKS, with the exception of the transition between optically thick and optically thin stages. From equation (4b), the definition of μ, and the relation $D = 206,265(R_{PN}/\theta)$ (where R_{PN} is the linear nebular radius in parsecs) we can determine the radius at which the PN becomes optically thin. For $\tau = 2.1$ we obtain $R_{PN} \sim 0.06$ pc. The same calculation to determine the PN radius at which the thick-to-thin transition occurs by using equation (3b) and $\tau = 3.13$ gives $R_{PN} \sim 0.09$ pc. The uncertainty in the determination of τ, and thus of R_{PN}, at the transition depends on the scatter of the ionized mass calibrators used in CKS. The new calibration is much more reliable.

The metallicities of the LMC and SMC are, on average, of the order of half and quarter that of the solar mix, respectively (Russell & Bessell 1989; Russell & Dopita 1990). The asymptotic giant branch (AGB) wind is likely to be dust driven; therefore, it has a strong dependence on metallicity. It is then expected that LMC and SMC stars with dust-driven winds lose smaller amounts of matter (Winters et al. 2000) during the AGB phase than their Galactic counterparts. The mass-loss history during the AGB determines the circumstellar density structure that will eventually constitute the PN shell (Villaver et al. 2002b). A reduced mass-loss rate during the AGB has the effect of decreasing the density of the circumstellar envelope prior of PN formation.

Furthermore, after the envelope is ejected, the remnant central star leaves the AGB and its effective temperature increases. The stellar remnant becomes a strong emitter of ionizing photons, responsible for ionizing the nebula. The mechanism that drives the wind during the central star phase (with velocities a few orders of magnitude higher than that experienced during the AGB phase) is the transfer of photon momentum to the gas through absorption by strong resonance lines (Pauldrach et al. 1988). The efficiency of this mechanism depends on metallicity, and thus it is expected to be less efficient in Magellanic Cloud central stars than in the Galactic ones, with correspondingly lower escape velocities for the winds and a decreased efficiency in shell snowplow.

As has been shown by Villaver et al. (2002a), the propagation of the ionization front determines the density structure of the nebula early in its evolution, while the pressure provided by the hot bubble has no effect at this stage. The propagation velocity of the Strömgren radius, which ultimately determines the transition from the optically thick to the optically thin stages, depends mainly on the ionizing flux from the star and on the density of the neutral gas. Given the dependence of the AGB mass-loss rates on metallicity, the ionization front will encounter a lower neutral density structure in Magellanic Cloud PNs than in Galactic PNs. This would tend to make the transition from optically thick to thin at a smaller radius in Magellanic Cloud PNs than in Galactic PNs. The fact that our Magellanic Cloud calibration of the CKS scale occurs at smaller radii than that derived by CKS is probably coincidence. On the other hand, if we really could determine empirically the transition radius as a function of metallicity, we would expect two different thick sequences for the SMC and the LMC PNs, given their different metallicity, and yet the sequences are almost identical (Figs. 1 and 2). That is, we do not see the effects of metallicity on our distance scale, and that is applicable to Galactic PNs as well. We discuss below (§ 4) how the newly derived distances match extremely well the best individual distances to Galactic PNs independently of metallicity.

4. COMPARISON OF OUR DISTANCE SCALE TO INDIVIDUAL GALACTIC PN DISTANCES

We have assessed that our new calibration of the PN distance scale is very similar to that of CKS, but with a revision in the transition between the radiation-bounded and the density-bounded stages. The comparison between the CKS and the SSV scales suffers from the fact that some of the CKS calibrators are obsolete, and that new Galactic calibrators have become available. It is worthwhile to compare the SSV scale with the best available individual distances to Galactic PNs to date before we confirm the validity of the new calibration.

In Table 2 we give the best set of individual Galactic PN distances available to date. Column (1) gives the common name; columns (2) and (3) give the best individual distance and, where available, its uncertainty; column (4) gives the parameter τ; columns (5) and (6) give the statistical distances for the same PN from CKS and SSV, respectively; and columns (7) and (8) give the distance determination method ("CM" for cluster membership, "P" for parallax, "E" for expansion, and "R" for reddening; see explanations below) and its reference. We have selected a sample of individual Galactic PN distances based on the literature, and whose statistical distances have been calculated by CKS and can be derived for the SSV calibration as well.

The best methods to get individual PN distances are (1) trigonometric parallax, (2) use of a spectroscopic companion of the PN central star, which allows derivation of the spectroscopic parallax, and (3) membership of the PN in an open or globular cluster. Apart from trigonometric parallaxes, which are applicable only for nearby PNs, the distance to the PN is that of a companion or a cluster, whose uncertainties are typically much lower than those related to other methods for PN distances. In the past decade there have been two major studies of PN parallaxes. C99 used *HST* imaging to determine central star companions of a PN sample, obtaining 10 probable associations and the relative spectroscopic parallaxes. We list all of these in Table 2, except for A31, where only a lower limit to the distance is given, and A33 and K1-27, whose distances seem to be controversial in C99. H07 published trigonometric parallaxes of several Galactic PNs. Following the discussion in H07, we include all their final determinations in Table 2, including the uncertainties. Planetary nebulae whose distances have been derived through cluster membership are the PN in Ps 1, whose distance has been recalculated by ABL00, and that in the open cluster NGC 2818, whose distance has been estimated by CHW03. Since CKS was published there have been other PNs observed in clusters, including Ja Fu 1 and Ja Fu 2 (Jacoby et al. 1997) and a PN in M22 (Monaco et al. 2004), but their distances are not included in Table 2 because either their cluster membership is not definitive or their nature is still uncertain, as described in detail in the discovery papers.

An alternative method for PN distances is the determination of the secular PN expansion, a method that had its renaissance with the use of the accurate relative astrometry afforded by *HST*. In this category we found distances to several PNs by Hajian et al. (1993, hereafter HTB93), HTB95, Hajian & Terzian (1996, hereafter HT96), Palen et al. (2002, hereafter P02), and Gomez et al. (1993, hereafter GRM93), and also the work by LL68. Among the distances determined by expansion we have only listed in Table 2 those deemed reliable by the authors listed above. In particular, in P02 there are several distances determined by different expansion algorithms, and if the results are very different by different methods for the same PN we have excluded them.

TABLE 2
Individual Distances of Galactic PNs

Name (1)	$D_{\rm ind}$ (pc) (2)	σ_D (pc) (3)	τ (4)	$D_{\rm CKS}$ (pc) (5)	$D_{\rm SSV}$ (pc) (6)	Method[a] (7)	Ref. (8)
A7	676	$^{+267}_{-150}$	6.28	216	218	P	H07
A24	521	$^{+112}_{-79}$	6.54	525	530	P	H07
A31	568	$^{+131}_{-90}$	6.97	233	235	P	H07
BD +30	2680	810	2.1	1162	3034	E	HTB93
HE 2−131	590	180	2.03	1413	3666	P	C99
IC 289	2190	1630	3.81	1434	1448	R	KL85
IC 1747	2450	1150	3.12	2937	2991	R	KL85
IC 2448	1410	640	3.17	3947	3984	E	P02
K1-14	3000	...	6.2	3378	3413	P	C99
K1-22	1330	...	6.45	988	997	P	C99
Mz 2	2160	...	3.85	2341	2363	P	C99
NGC 1535	2310	...	3.31	2283	2305	P	C99
NGC 2392	1600	130	3.93	1247	1258	E	LL68
NGC 2452	3570	560	3.81	2811	2838	R	GPP86
NGC 2792	1910	220	3.16	3021	3050	R	GPP86
NGC 2818	1855	200	4.69	1979	1998	CM	CHW03
NGC 3132	770	...	3.94	1251	1263	P	C99
NGC 3211	1910	500	3.51	2873	2901	R	GPP86
NGC 3242	420	160	3.22	1083	1094	E	HTB95
NGC 3918	2240	840	2.62	1010	1639	R	GPP86
NGC 5189	1730	530	4.59	540	546	R	GPP86
NGC 5315	2620	1030	1.94	1242	3177	R	GPP86
NGC 6210	1570	400	3.01	2025	2281	E	HTB95
NGC 6302	1600	600	2.77	525	741	E	GRM93
NGC 6565	1000	440	3.29	4616	4660	R	GPP86
NGC 6567	1680	170	2.68	2367	3610	R	GPP86
NGC 6572	703	95	2.16	705	1736	E	HTB95
NGC 6720	704	$^{+445}_{-196}$	4.1	872	880	P	H07
NGC 6741	1540	770	2.49	2047	3727	R	KL85
NGC 6853	379	$^{+54}_{-42}$	4.94	262	264	P	H07
NGC 6894	1090	110	4.5	1653	1669	R	KL85
NGC 7009	1400	...	3.03	1201	1325	E	S04
NGC 7026	1450	840	2.91	1902	2352	R	KL85
NGC 7027	790	...	1.46	273	632	P	HTB95
NGC 7293	219	$^{+27}_{-21}$	5.7	157	159	P	H07
NGC 7354	2460	1440	2.83	1271	1697	R	KL85
NGC 7662	790	750	2.57	1163	1962	E	HT96
PS 1	1.23E4	600	2.93	8380	1.0E4	CM	ABL00
Pw We 1	365	$^{+47}_{-37}$	7.83	141	416	P	H07
Sp 3	2380	...	4.32	1877	1895	P	C99

[a] P: Parallax; CM: cluster membership; E: expansion; R: reddening.

References.—(ABL00) Alves et al. 2000; (CHW03) Chen et al. 2003; (C99) Ciardullo et al. 1999; (GPP86) Gathier et al. 1986; (GRM93) Gomez et al. 1993; (HT96) Hajian & Terzian 1996; (HTB93) Hajian et al. 1993; (HTB95) Hajian et al. 1995; (H07) Harris et al. 2007; (KL85) Kaler & Lutz 1985; (LL68) Liller & Liller 1968; (P02) Palen et al. 2002; (S04) Sabbadin et al. 2004.

Uncertainties in expansion distances, when available, are much higher than those of parallaxes or cluster membership, and the method is intrinsically less reliable, given the impossibility of following the PN acceleration history, and the modeling difficulty given unknown processes such as differential mass loss.

Finally, a very rough individual distance can be derived in some cases by studying the reddening patches around the PN and then building reddening-distance plots for the known stars surrounding the PN. This method, although providing several data points in the literature, is the most uncertain given the inhomogeneity of the Galactic interstellar medium. GPP86 derived reddening distances for several PNs, and we used in Table 2 only the reliable ones, as deemed by the authors. We have excluded NGC 2346, since the scatter in its distance-reddening plot is overly large. KL85 also

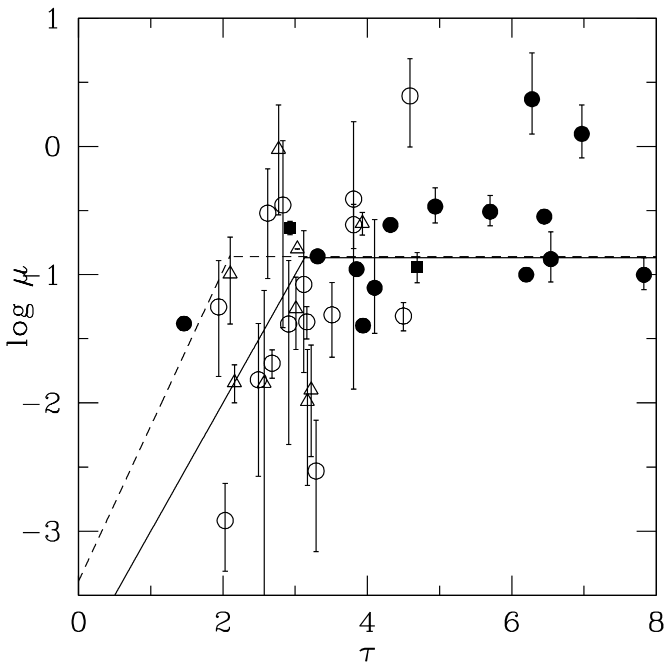

FIG. 4.—Galactic PNs of known distances plotted on the τ–log μ plane. Lines are as in Fig. 2. Symbols denote the method used for individual distance determination: P (*filled circles*), CM (*filled squares*), R (*open circles*), and E (*open triangles*).

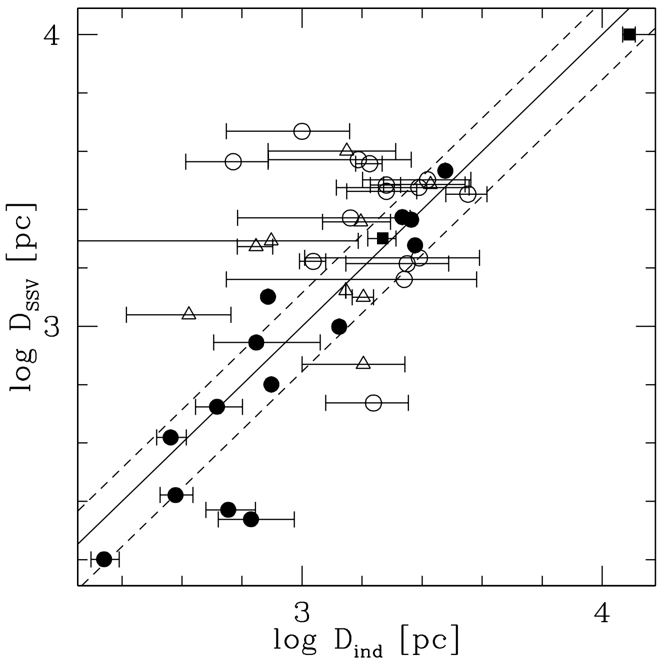

FIG. 5.—Comparison of statistical distances form our new calibration (SSV) with the individual distances in Table 2. Symbols represent the individual distance determination method, as in Fig. 4. The solid line shows 1:1 correspondence. Dashed lines represent the 30% differences between statistical and individual distances.

published several PN distances by the same method, and we included their results in Table 2.

In Figure 4 we plot the data of Table 2 on the τ–log μ plane, drawing also the CKS and the SSV distance scales (note that the scales of Figs. 3 and 4 are different). It is interesting to note that the best data points, those of the PNs whose distances have been determined via parallax or cluster membership, follow very well the SSV calibration, and they are less compatible with that of CKS. Naturally, the CKS calibration was based principally on reddening and expansion distances, since very few parallaxes were available at that time, and we can see that the thinning sequence determined by the data points relative to expansion or reddening distances is compatible with the CKS calibration (but these individual distances have much lower reliability than the parallaxes and cluster memberships represented by the filled symbols). While the SSV seems to be the best statistical scale to be used for Galactic PNs, its preference, for optically thick PNs, over the CKS scale is based only on one data point (the parallax at $\tau < 2.1$). But let us recall here that the filled symbols *are not* the calibrators of the SSV scale; rather, they are the Galactic PNs with best individual distances to date, used for comparison, while the calibration is based on $\sim$70 data points whose error bars would be smaller than the symbols.

In Figure 5 we show the direct comparison of the individual PN distances and those from the SSV calibration, where the correspondence of the parallax and cluster membership individual distances with the SSV distances is remarkable. It is worth noting that the two lower left filled circles, those for which the parallax and statistical distances do not coincide within 30%, are A7 and A31; both are very large nebulae, whose diameters are larger than the radio beam used to detect the 5 GHz flux (Milne 1979) and whose flux densities are deemed to be uncertain. In Figure 6 we show the distribution of the relative differences of the SSV and individual distances versus τ for the four methods of deriving individual distances. The thin vertical lines represent $\tau = 2.1$ and 3.1, i.e., the thick-to-thin PN transition for the CKS and SSV scales. We could conclude that the SSV scale fails to reproduce the individual distances for PNs around the transition between thick and thin, but this failure seems to pertain only to the comparison with expansion and reddening distances, and it does not occur for the comparison with parallax and cluster membership distances.

5. COMPARISON OF STATISTICAL DISTANCE SCALES

We compare the relative merits of the new SSV scale, calibrated on Magellanic Cloud PNs, in relation to other distance scales in the literature. We compare the statistical distances from different methods to individual Galactic PN distances, by using only the best individual PN distances of Table 2, those from parallax and cluster membership. We also calculate the distances to all LMC and SMC PNs using the statistical methods, then we compare the resulting averages with the actual distances to the Magellanic Clouds. It is worth recalling that all old scales have been calibrated with Galactic or bulge PNs; thus, we expect a lower reproducibility of the Magellanic Cloud distances.

For all scales we give the following in Table 3: in column (1) the reference, in column (2) the statistical method, in column (3) the correlation coefficient between statistical and individual PN distances, in column (4) the mean relative difference between the statistical and individual distances, in column (5) the relative difference between the median distances to Large Magellanic Cloud PNs and the actual LMC distance, and in column (6) the same relative difference, but for the SMC PNs. Statistical distance scales in the literature used in this comparison are those by CKS, vdSZ95, Z95, SB96, and BL01.

The statistical scheme that best compares with the best individual distances is the SSV scale, which has higher ($R_{xy} = 0.99$) correlation and lower median difference between statistical and individual distances than any other scale, and which best reproduces the Magellanic Cloud distances. This is hardly a surprise, since for the first time it was possible to calibrate a distance scale

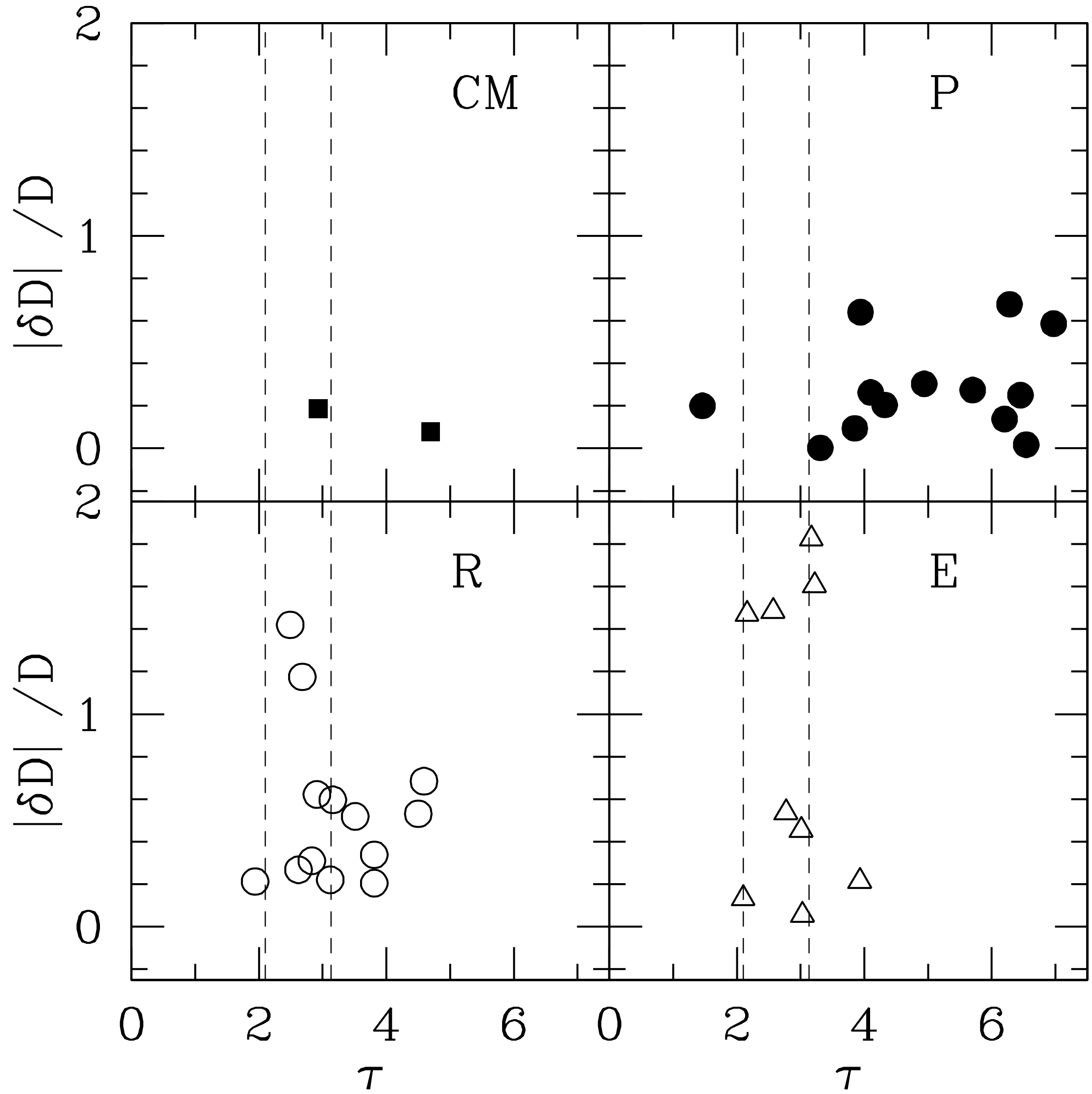

FIG. 6.—Relative differences between SSV statistical and individual PN distances, as a function of τ, separated in the panels by individual distance method. Symbols are as in Fig. 4. Vertical lines denotes the τ of the thick-to--thin transition for the CKS and the SSV scales.

TABLE 3

COMPARISON OF STATISTICAL AND INDIVIDUAL DISTANCES

Reference (1)	Method (2)	R_{xy} (3)	$\langle \delta D/D \rangle_{\rm Gal}$ (4)	$(\langle D_{\rm stat} \rangle - D_{\rm LMC})/D_{\rm LMC}$ (5)	$(\langle D_{\rm stat} \rangle - D_{\rm SMC})/D_{\rm SMC}$ (6)
SSV	μ-τ	0.99	0.26	0.01	0.01
Old Scales					
CKS	μ-τ	0.97	0.32	0.04	0.05
vdSZ95	$\log T_b$–$\log R_{\rm PN}$	0.74	0.86	0.13	0.12
Z95	$\log M_{\rm ion}$–$\log R_{\rm PN}$	0.70	1.10	0.19	0.22
BL01	$\log M_{\rm ion}$–$\log R_{\rm PN}$	0.61	1.35	0.12	0.12
SB96	$\log I$–$\log R_{\rm PN}$	0.95	0.46	0.02	0.02
LMC/SMC Calibrations					
This paper	$\log T_b$–$\log R_{\rm PN}$	0.82	0.74	0.07	0.02
	$\log M_{\rm ion}$–$\log R_{\rm PN}$	0.80	0.72	0.11	0.08
	$\log I$–$\log R_{\rm PN}$	0.96	0.36	0.03	0.02

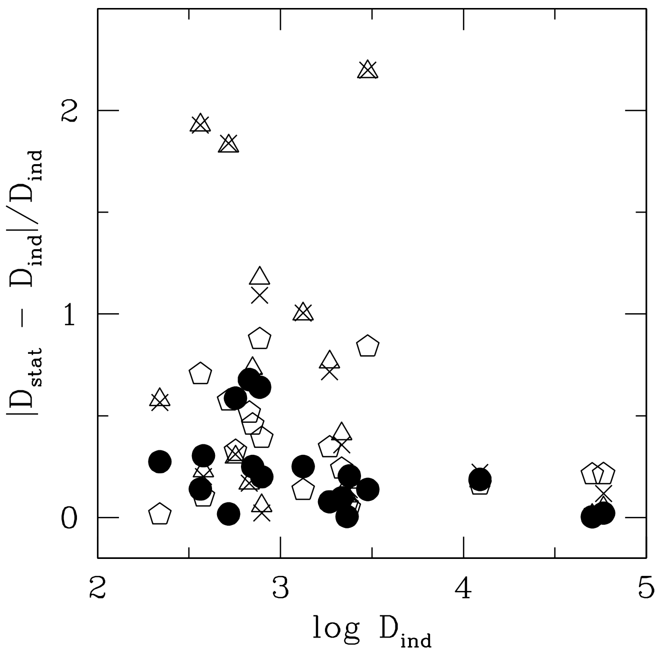

FIG. 7.—Relative differences between statistical and individual PN distances, plotted against the individual distances, for the Magellanic Cloud PN-calibrated scales of CKS (*filled circles*), vdSZ95 (*triangles*), BL01 (*crosses*), and SB96 (*pentagons*).

with absolute calibrators from the Magellanic Clouds. By comparison, the correlation coefficients between the distances from the CKS, vdSZ95, Z95, SB96, and BL01 scales are always lower, and the median of the relative differences are higher.

We also want to test whether PN distances derived with other distance scales, if recalibrated with the Magellanic Cloud PNs, would compare better than the SSV scale to the best individual distances of Galactic PNs. First, we consider the relation between the brightness temperature and the linear nebular radius, which vdSZ95 calibrated with Galactic bulge PNs. Our new calibration of the relation is

$$\log D(T_b) = 3.49 - 0.35 \log \theta - 0.32 \log F, \qquad (5)$$

based on a fit of the $\log T_b$–$\log R_{\rm PN}$ relation [$R_{\rm PN} = (\theta D)/206,265$]. We also calibrated the $\log M_{\rm ion}$–$\log R_{\rm PN}$ relation as in Maciel & Pottasch (1980), Z95, and BL01 and found, by assuming that the filling factor is 0.6,

$$\log D(M_{\rm ion}) = 3.45 - 0.34 \log \theta - 0.33 \log F. \qquad (6)$$

Finally, we also recalibrated with the Magellanic Cloud PNs the relation between the surface brightness, $I = F/(\pi\theta^2)$, and $R_{\rm PN}$, as in SB96, and obtained

$$\log D(I) = 3.68 - 0.50 \log \theta - 0.25 \log F. \qquad (7)$$

The possibility of building a distance scale based on a $\log I$–$\log R_{\rm PN}$ calibration was mentioned by Stanghellini et al. (2002) and also used by Jacoby et al. (2002).

All three relations used to derive the distance scales in equations (5), (6), and (7) have high correlation coefficients ($R_{xy} \sim 0.8$). In these relations, excluding the bipolar PNs does not change the coefficients by more than 5%, and thus their exclusion as calibrators is irrelevant.

Using the scales in equations (5), (6), and (7) we have calculated the distances for those Galactic PNs whose individual distances are known either through a trigonometric or spectroscopic parallax or by cluster membership. In Table 3 we give the comparison between these newly calibrated scales and the individual distances of PNs. We also give the estimates for the LMC and SMC distances, and we infer that the SSV scale is superior to all other scales here recalibrated with the Magellanic Cloud PNs as well. We then plot in Figure 7 the relative difference between the statistical and individual distances for the scales recalibrated with Magellanic Cloud PNs. The filled circles represent the SSV scale, triangles are the distances from the T_b-$R_{\rm PN}$ relation (eq. [5]), crosses represent the $\log M_{\rm ion}$–$\log R_{\rm PN}$ scale (eq. [6]), and pentagons are the distances from equation (7), based on the $\log I$–$\log R_{\rm PN}$ relation. We see that the SSV scale is the best possible Galactic statistical distance scale with the calibrators and comparisons available to date. Since the $\log I$–$\log R_{\rm PN}$ relation works for bipolar PNs, it might be used to determine the distance to bipolar PNs instead of the SSV scale.

6. CONCLUSION

The wealth of new data available that describe the physical parameters of Magellanic PNs has allowed us to check and recalibrate the Shklovsky/Daub/CKS statistical distance scale, which is most commonly used in the literature, and provide distances of 645 Galactic PNs following the new distance scale calibration (Table 1). To calculate the SSV distance for other PNs, or for the same PNs but using parameters other than those in CKS, given θ and F, the 5 GHz flux, one can use the following equations:

$$\log D_{\rm SSV} = 3.06 + 0.37 \log \theta - 0.68 \log F, \quad \tau < 2.1, \qquad (8a)$$

$$\log D_{\rm SSV} = 3.79 - 0.6 \log \theta - 0.2 \log F, \quad \tau > 2.1. \qquad (8b)$$

If the 5 GHz flux is not available for the given PN, one can use equation (6) in CKS to derive the equivalent 5 GHz flux from the Hβ flux.

In this paper we have used recent data on PNs in the Magellanic Clouds to construct a set of calibrators for which the distances are known to high absolute accuracy ($\sim$10%), and for which the dispersion among the distances is extraordinarily small (a few percent). Furthermore, the great distance of these nebulae allows us to establish a distance scale factor that is insensitive to uncertainties in distances to Galactic PNs that are drawn from a heterogeneous, nearby (few hundred parsecs) sample; a local sample has generally been necessary given the limited range over which many independent distance methods (notably trigonometric and expansion parallaxes) can provide accurate distances. In addition, we use consistent and reliable means to determine angular sizes (from photometric radii), and the Hβ fluxes and extinction constants, derived from *HST* calibrations, are among the most reliable in the literature. There has never been a better set of calibrators for statistical distance determinations. For comparison, we selected Galactic PNs for which the independent distances are the best available (including recently published data), and we evaluated the reliability of various independent distance methods by the degree to which they are consistent with our distance scale.

With this study we show the following: (1) The distance scale as calibrated from the Magellanic Cloud PNs is very similar to that derived by CKS. (2) Our revised distance scale agrees superbly with the most accurate distances measured for individual Galactic PNs. We also show that other methods of statistical distance determination generally do not yield results that are better than this statistical method. (3) The distance scale does not work for PNs with bipolar morphology, and we believe this is because progenitors of bipolars are often not fully ionized during the course of PN evolution (the log I–log R_{PN} relation could be used instead for these PNs). (4) With the Magellanic Cloud calibration we provide a more robust physical basis for why the Shklovsky/Daub distance scale works, despite wide variations in the expected ionized mass; we also show that the recalibration of other distance scales with Magellanic Cloud PNs might not work as well as the recalibrated Shklovsky/Daub distance scale. (5) The dispersion in the distance scale is an inherent property of the method and cannot be reduced significantly by using better calibrators. (6) The radiation-bounded sequence for Magellanic Cloud PNs may terminate at higher surface brightness than previously derived. It seems that the new sequence and the radiation-bounded to density-bounded transition does not depend on metallicity very much, as it is the same for the LMC and the SMC PNs; the best available data show that the Magellanic Cloud calibration of this sequence is entirely consistent with Galactic PNs.

Many thanks to Bruce Balick for a scientific discussion on the importance of the PN distance scale, and an anonymous referee for giving suggestions that improved the paper.

REFERENCES

Acker, A., Marcout, J., Ochsenbein, F., Stenholm, B., & Tylenda, R. 1992, The Strasbourg-ESO Catalogue of Galactic Planetary Nebulae (Garching: ESO)
Alves, D. R., Bond, H. E., & Livio, M. 2000, AJ, 120, 2044 (ABL00)
Benedict, G. F., et al. 2002, AJ, 123, 473
Bensby, T., & Lundström, I. 2001, A&A, 374, 599 (BL01)
Cahn, J. H., Kaler, J. B., & Stanghellini, L. 1992, A&AS, 94, 399 (CKS)
Chen, L., Hou, J. L., & Wang, J. J. 2003, AJ, 125, 1397 (CHW03)
Ciardullo, R., Bond, H. E., Sipior, M. S., Fullton, L. K., Zhang, C.-Y., & Schaefer, K. G. 1999, AJ, 118, 488 (C99)
Crowl, H. H., Sarajedini, A., Piatti, A. E., Geisler, D., Bica, E., Clariá, J. J., & Santos, J. F. C. 2001, AJ, 122, 220
Daub, C. T. 1982, ApJ, 260, 612 (D82)
Feast, M. W. 1989, in Recent Developments of Magellanic Cloud Research, ed. K. S. de Boer, F. Spite, & G. Stasinska (Paris: Obs. Paris), 75
Freedman, W. L., et al. 2001, ApJ, 553, 47
Freeman, K. C., Illingworth, G., & Oemler, A. 1983, ApJ, 272, 488
Gathier, R., Pottasch, S. R., & Pel, J. W. 1986, A&A, 157, 171 (GPP86)
Gomez, Y., Rodriguez, L. F., & Moran, J. M. 1993, ApJ, 416, 620 (GRM93)
Hajian, A. R., & Terzian, Y. 1996, PASP, 108, 258 (HT96)
Hajian, A. R., Terzian, Y., & Bignell, C. 1993, AJ, 106, 1965 (HTB93)
———. 1995, AJ, 109, 2600 (HTB95)
Harris, H. C., et al. 2007, AJ, 133, 631 (H07)
Jacoby, G. H., Feldmeier, J. J., Claver, C. F., Garnavich, P. M., Noriega-Crespo, A., Bond, H. E., & Quinn, J. 2002, AJ, 124, 3340
Jacoby, G. H., Morse, J. A., Fullton, L. K., Kwitter, K. B., & Henry, R. B. C. 1997, AJ, 114, 2611
Kaler, J. B., & Lutz, J. H. 1985, PASP, 97, 700 (KL85)
Liller, M. H., & Liller, W. 1968, in IAU Symp. 34, Planetary Nebulae, ed. D. E. Osterbrock & C. R. O'Dell (Dordrecht: Reidel), 38 (LL68)
Maciel, W. J. 1984, A&AS, 55, 253
Maciel, W. J., & Pottasch, S. R. 1980, A&A, 88, 1
Milne, D. K. 1979, A&AS, 36, 227
Monaco, L., Pancino, E., Ferraro, F. R., & Bellazzini, M. 2004, MNRAS, 349, 1278
Mould, J. R., et al. 2000, ApJ, 529, 786
Palen, S., Balick, B., Hajian, A. R., Terzian, Y., Bond, H. E., & Panagia, N. 2002, AJ, 123, 2666 (P02)
Pauldrach, A., Puls, J., Kudritzki, R. P., Mendez, R. H., & Heap, S. R. 1988, A&A, 207, 123
Russell, S. C., & Bessell, M. S. 1989, ApJS, 70, 865
Russell, S. C., & Dopita, M. A. 1990, ApJS, 74, 93
Sabbadin, F., Turatto, M., Cappellaro, E., Benetti, S., & Ragazzoni, R. 2004, A&A, 416, 955 (S04)
Schneider, S. E., & Buckley, D. 1996, ApJ, 459, 606 (SB96)
Shaw, R. A., Stanghellini, L., Mutchler, M., Balick, B., & Blades, J. C. 2001, ApJ, 548, 727
Shaw, R. A., Stanghellini, L., Villaver, E., & Mutchler, M. 2006, ApJS, 167, 201
Shklovsky, I. S. 1956a, Astron. Zh., 33, 222
———. 1956b, Astron. Zh., 33, 315
Stanghellini, L., Shaw, R. A., Balick, B., Mutchler, M., Blades, J. C., & Villaver, E. 2003, ApJ, 596, 997
Stanghellini, L., Shaw, R. A., Mutchler, M., Palen, S., Balick, B., & Blades, J. C. 2002, ApJ, 575, 178
van der Marel, R. P., & Cioni, M. L. 2001, AJ, 122, 1807
van de Steene, G. C., & Zijlstra, A. A. 1995, A&A, 293, 541 (vdSZ95)
Villaver, E., García-Segura, G., & Manchado, A. 2002a, ApJ, 571, 880
Villaver, E., Manchado, A., & García-Segura, G. 2002b, ApJ, 581, 1204
Westerlund, B. E. 1997, The Magellanic Clouds (Cambridge: Cambridge Univ. Press)
Winters, J. M., Le Bertre, T., Jeong, K. S., Helling, C., & Sedlmayr, E. 2000, A&A, 361, 641
Zhang, C. Y. 1995, ApJS, 98, 659 (Z95)